ACS Catalysis

Research Article

pubs.acs.org/acscatalysis

Wettability-Driven Palladium Catalysis for Enhanced Dehydrogenative Coupling of Organosilanes

Jian-Dong Lin,[†] Qing-Yuan Bi,[‡] Lei Tao,[†] Tao Jiang,[†] Yong-Mei Liu,[†] He-Yong He,[†] Yong Cao,*[,†] and Yang-Dong Wang*[,§]

[†]Shanghai Key Laboratory of Molecular Catalysis and Innovative Materials, Department of Chemistry, Fudan University, Shanghai 200433, People's Republic of China

[‡]State Key Laboratory of High Performance Ceramics and Superfine Microstructures, Shanghai Institute of Ceramics, Chinese Academy of Sciences, Shanghai 200050, People's Republic of China

[§]SINOPEC Shanghai Research Institute of Petrochemical Technology, Shanghai 201208, People's Republic of China

S *Supporting Information*

ABSTRACT: Direct coupling of Si−H bonds has emerged as a promising strategy for designing chemically and biologically useful organosilicon compounds. Heterogeneous catalytic systems sufficiently active, selective, and durable for dehydrosilylation reactions under mild conditions have been lacking to date. Herein, we report that the hydrophobic characteristics of the underlying supports can be advantageously utilized to enhance the efficiency of palladium nanoparticles (Pd NPs) for the dehydrogenative coupling of organosilanes. As a result of this prominent surface wettability control, the modulated catalyst showed a significantly higher level of efficiency and durability characteristics toward the dehydrogenative condensation of organosilanes with water, alcohols, or amines in comparison to existing catalysts. In a broader context, this work illustrates a powerful approach to maximize the performance of supported metals through surface wettability modulation under catalytically relevant conditions.

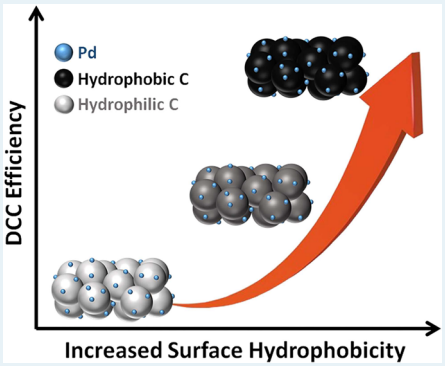

KEYWORDS: *dehydrocoupling, organosilanes, Pd nanoparticles, heterogeneous catalysis, hydrophobicity*

1. INTRODUCTION

The search for new, robust solid catalysts for selective chemical processes has spurred the onset of meticulous design strategies along with ingenious synthesis of active phases (i.e., active sites).[1] Alternatively, a facile and more straightforward approach for catalyst tailoring lies in modulating surface wettability such that the substrate−catalyst interaction can be favorably manipulated in a targeted and controlled manner.[2] In this sense, one of the most elegant examples is the enhanced activity and selectivity of hydrophobic titanosilicate (TS-1) for the catalytic oxidation of organic compounds using aqueous H_2O_2 as a terminal oxidant.[3] Recent progress in the understanding of zeolite and zeotype solid acid materials with controlled wettability has led to the successful development of a plethora of benign acid-catalyzed processes for the production of renewable chemicals within the biorefinery context.[4] Surprisingly, the potential offered by wettability control in regulating the characteristics of supported metal catalysts has remained largely unexplored,[2c] despite the paramount importance of these materials in enabling various imperative catalytic processes.

Dehydrogenative cross-coupling (DCC) reactions have emerged as a promising tool to precisely construct new C−X and X−X (X = heteroatom) bonds via direct C−H or X−H activation.[5] In this sense, organosilanes constitute attractive DCC reagents to access various functionalized organosilicon compounds serving as both highly useful building blocks and key intermediates for polymeric and other advanced organic materials.[6] To date, several efficient DCC strategies for silanes using hydrogen acceptors (i.e., oxidants) such as hydrogen peroxide and molecular oxygen have been developed.[7] From the viewpoint of atom efficiency and safety perspectives, an acceptor-free approach would be ideal. Advantageously, this may also provide a convenient route for simultaneous H_2 generation and storage.[6d] However, with the aim of maximizing the efficiency of organosilanes as DCC reagents, the inherently sluggish kinetics for Si−H cleavage must be circumvented.[8] While several efficient homogeneous catalysts have been developed,[9] the corresponding heterogeneous catalysts have generally displayed significantly lower efficiencies despite the large number of attempts.[10] With the aim of overcoming these issues, highly robust solid catalysts able to significantly improve the reaction kinetics under moderate conditions are thus urgently required.

Metallic palladium (Pd) is commonly used as an active component in hydrolytic oxidation of organosilanes or

Received: November 14, 2016
Revised: January 4, 2017
Published: January 23, 2017

DOI: 10.1021/acscatal.6b03233
ACS Catal. 2017, 7, 1720−1727

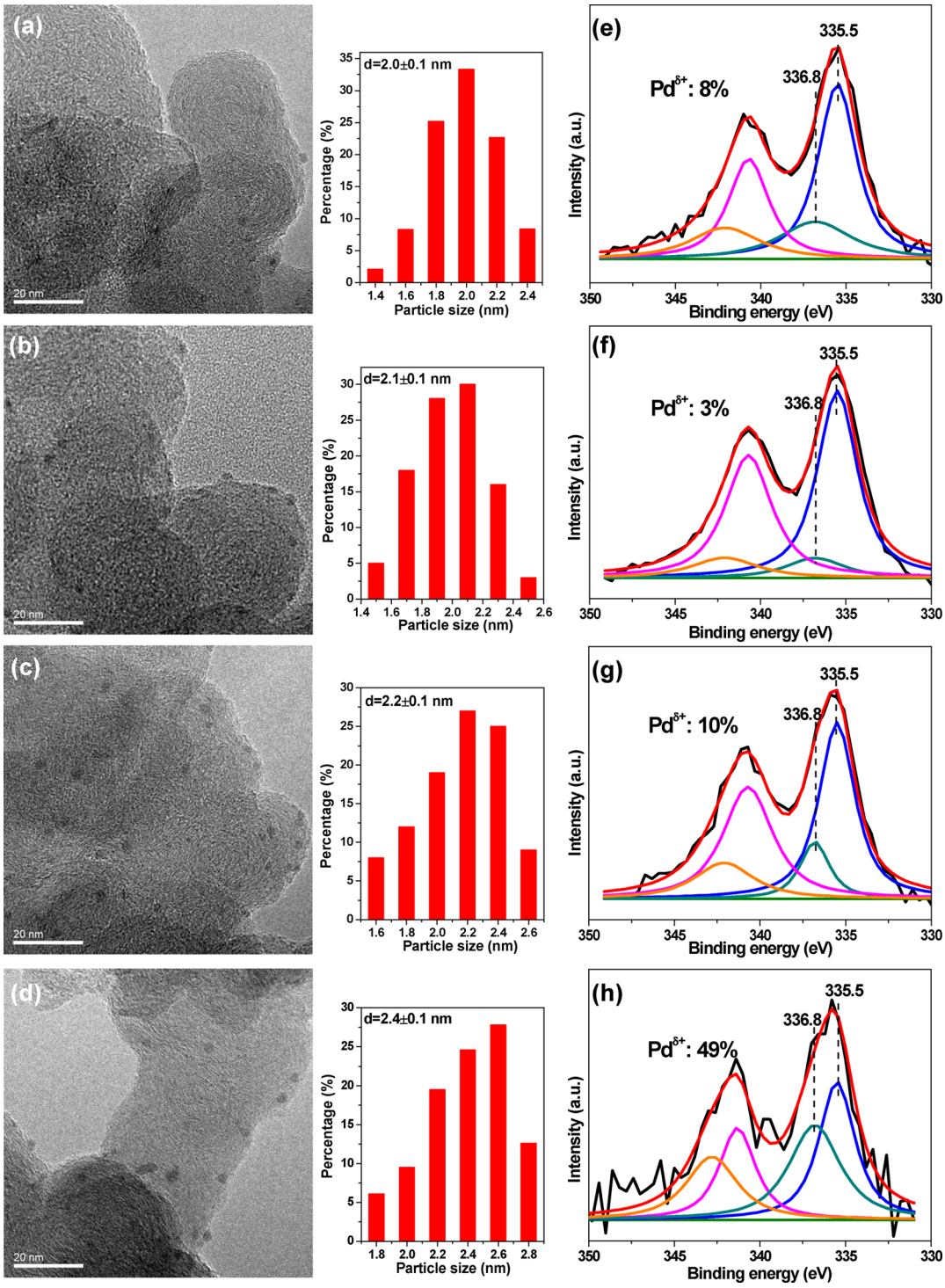

Figure 1. Transmission electron microscopy (TEM) images, particle distribution, and Pd 3d XP spectra of: (a, e) Pd/XC-72, (b, f) Pd/XC-72-700-Ar, (c, g) Pd/XC-72-HNO_3, and (d, h) Pd/XC-72-700-Ar stored for 2 years.

dehydrogenative silylation of alcohols at low temperature and under additive-free conditions.[10a−c,14a] However, heterogeneous Pd-based catalysts are typically limited by the low affinity interaction between organosilanes and water or alcohols, which hinders the efficiency of the desired transformation process.[10a,b] Engineering metal−support interfaces displaying strong enough interactions with the reactants while weakly interacting with the products would offer an opportunity for enhanced catalytic efficiencies.[2c,11] Although many studies have focused on regulating the electronic structure of the supported Pd or deliberately increasing the hydrophilic properties of the underlying supports,[10a−d,f−h,j−l,n] a catalyst outperforming the state of the art homogeneous systems still remains elusive. We report, for the first time, that the use of highly hydrophobic carbon black (CB) as a support material can significantly enhance the efficiency of Pd nanoparticles (NPs) for dehydrogenative coupling of organosilanes. As a result of a noticeable surface wettability modulation, the engineered catalyst showed exceedingly enhanced activity and durability

DOI: 10.1021/acscatal.6b03233
ACS Catal. 2017, 7, 1720−1727

toward dehydrogenative condensation of organosilanes with water, alcohols, or amines in comparison to existing catalysts.

2. RESULTS AND DISCUSSION

To begin our studies on direct coupling of Si−H bonds via hydrolytic oxidation, we selected a series of commercial CB as a supporting material for Pd NPs, anticipating that the inherent hydrophobic nature of these materials would have a positive effect on the outcome of the reaction.[12] In an effort to explore and evaluate the possible wettability effects via surface engineering, we opted for a systematic approach to progressively impart surface hydrophobicity on the modified CB materials.[12b] This was achieved by subjecting the as-received commercial CB materials to an inert gas annealing treatment at elevated temperatures (for details, see the Supporting Information). Analysis by water and organosilane adsorption revealed an increased hydrophobicity in the sample exposed to temperatures above 300 °C, in contrast to the material treated with 32% HNO_3, which was shown to be particularly effective for generating a highly hydrophilic surface (ca. 5-fold increase in water adsorption along with an 8-fold decrease in organosilane adsorption; Table S3 in the Supporting Information). Essentially, the increased hydrophobicity was associated with a lower number of surface oxygenated species, as revealed by infrared and X-ray photoelectron spectroscopy (XPS) analysis (Figures S2 and S3 in the Supporting Information). Subsequent wet-chemical reductive processing[13] of these wettability-modulated CB materials led to their decoration with narrowly size distributed Pd NPs (average size ca. 2 nm) having basically similar chemical states and metal−support interface structures (Figure 1 and Figure S1 in the Supporting Information) on the surface of the carbon supports.

Initial experiments dealing with the hydrolysis of triethylsilane (**1a**) in THF at 25 °C were promising and suggested that CB-supported Pd NPs could certainly perform very well (Table 1, entries 1−4). The assessment of a number of CB structures revealed that surface-engineered Vulcan XC-72 carbons were particularly effective support classes, with the highly hydrophobic XC-72-700-Ar (obtained via annealing at 700 °C under an Ar atmosphere) providing an outstanding dehydrogenative silylation efficiency with the exclusive production of triethylsilanol (**1b**) as a result of the reaction (Table 1, entries 5−7). As an illustration of the efficiency of XC-72-700-Ar as a support, Pd/XC-72-700-Ar with a palladium content of 1.0 wt % achieved complete hydrolysis of **1a** within 1 min at a substrate to catalyst (S/C, $mol_{sub.}/mol_{Pd}$) ratio of 10000, with a turnover frequency (TOF) of 1.6×10^6 h^{-1} for quantitative **1a** hydrolysis on the basis of surface Pd atoms (Table 1, entry 6). This catalytic system showed fast kinetics while maintaining its activity for an extended period of time, as inferred by monitoring the H_2 release upon sequential injection of **1a** at intervals into a THF−H_2O solution containing Pd/XC-72-700-Ar.[9d] This result was remarkable and became more relevant as the H_2 gas produced using Pd/XC-72-700-Ar was easily controlled by slowly and continuously injecting **1a** into the catalytic system (Figure S4 in the Supporting Information). Furthermore, this system also worked well under scale-up conditions (see the Supporting Information). For example, 50 mmol of **1a** was successfully transformed into **1b** in nearly quantitative yield (>99%). In this case, the recovered Pd/XC-72-700-Ar material was reused at least 10 times while maintaining its initial activity (i.e., the total turnover number (TON) approached 8.0×10^5; Figure S5 in the Supporting Information). To the best of our knowledge, this result is far superior to any reported example of the hydrolytic oxidation of organosilanes (Table S8 in the Supporting Information).[9,10]

Table 1. Study of CB-Supported Pd Catalysts for the Dehydrocoupling of 1a and H_2O[a]

$Et_3Si–H$ (**1a**) + H_2O → H_2 + $Et_3Si–OH$ (**1b**)

entry	catalyst[b]	time (s)	yield (%)	TOF (h^{-1})[c]
1	Pd/XC-72	72	>99	510800
2	Pd/BP2000	119	97	299900
3	Pd/M800	90	97	396800
4	Pd/660R	146	98	247100
5	Pd/XC-72-300-Ar	63	>99	583600
6	Pd/XC-72-700-Ar	57	>99	645300 (1686000[d])
7	Pd/XC-72−900-Ar	59	>99	623400
8	XC-72-700-Ar	720	nd	
9[e]	Pd/XC-72-700-Ar	720	nd	
10[f]	Pd/XC-72-700-Ar	62	99	588700
11	Pd/XC-72-HNO_3	980	95	35260
12[g]	Pd/XC-72-HNO_3-400-Ar	470	96	75540

[a]Reaction conditions unless specified otherwise: 5 mmol of **1a**, 0.5 mL of water, 10 mL of THF, S/C = 10000, air atmosphere, 25 °C. nd = not detected. [b]The Pd loading was 1.0 wt %. [c]Based on total Pd atoms. [d]Based on surface Pd atoms; the dispersion was calculated from CO chemisorption measurements. [e]Reaction conditions: 5 mmol of **1a**, 10 mL of dried THF, S/C = 10000, 25 °C. [f]The catalyst was stored for 2 years under ambient conditions. [g]The catalysts was obtained after post heat treatment of Pd/XC-72-HNO_3 under an Ar atmosphere.

Notably, this hydrolytic oxidation proceeded very efficiently even under subambient temperatures, although the reaction rate significantly increased with temperature (Table S1 in the Supporting Information). The apparent activation energy (E_a) was estimated to be 38.9 kJ mol^{-1} (Figure S6 in the Supporting Information), which is lower in comparison to the values for most of the previously reported systems.[9f−h] The control experiments showed no reaction at all in the absence of Pd species or in dried THF under identical conditions (Table 1, entries 8 and 9), thereby confirming that the Pd species serve as the active sites for this reaction and the H_2 gas is formed from **1a** and water (i.e., water provides one H atom). With the aim of gaining a better understanding of the nature of the catalytically active sites, a Pd/XC-72-700-Ar sample stored in air for a 2 year period was evaluated. Interestingly, the catalytic activity remained nearly unchanged (Table 1, entry 10, and Figure S7 in the Supporting Information), although the relative fraction of surface PdO in the air-stored sample, as confirmed by XPS, was significantly larger in comparison to its freshly prepared counterpart (Figure 1h). This result excludes the possibility of the particular surface chemical state of Pd NPs markedly influencing the activity, in contrast to recent studies underlining the positive role of surface oxygenated Pd species on the efficiency of the anaerobic hydrolytic oxidation of organosilane.[10b,c]

Apart from CB, various other carbon nanostructures were also evaluated as supporting matergials for the hydrolysis of **1a**. As shown in Table S2 in the Supporting Information, Pd deposited on carbon nanotubes (CNTs), activated carbon (AC), and reduced graphene oxide (GO) nanosheets showed very poor performance under identical reaction conditions, although the content, shape, and size of the Pd species in these

DOI: 10.1021/acscatal.6b03233
ACS Catal. 2017, 7, 1720−1727

samples were similar to those of Pd/XC-72-700-Ar (Figure S1 in the Supporting Information). It should be mentioned that Pd loaded on the hydrophilic surface of modified XC-72-HNO_3 also showed very low activity toward hydrolysis of **1a** (Table 1, entry 11). All of these observations indicate that the hydrophobicity of the underlying support plays a key role in achieving high dehydrocoupling capability in this process. With the aim of clarifying the role of the support wettability, the rate dependence on the substrate concentration was studied. The reaction orders with respect to **1a** were 0.0 and +0.51 for Pd/XC-72-700-Ar and Pd/XC-72-HNO_3 (Figure S8 in the Supporting Information), respectively, thereby indicating that the substrate was more strongly adsorbed on the surface of Pd/XC-72-700-Ar, and this tendency was also supported by comparing the amount of adsorbed **1a** for all of the catalysts examined (Table S3 in the Supporting Information).

The important role of support wettability in facilitating the above Pd-mediated catalysis is further highlighted by the fact that a dramatic enhancement of catalytic activity can be achieved by subjecting the hydrophilic Pd/XC-72-HNO_3 sample to a post heat treatment under an inert atmosphere (Table 1, entry 12). In line with the pristine CB material case, annealing the Pd/XC-72-HNO_3 smaple at elevated temperatures also leads to an effective removal of oxygen-containing surface functional groups, as verified by the IR analysis as well as the organosilane and water adsorption data (Figure S2 and Table S3 in the Supporting Information). Additioal TEM measurements shown in Figure S1 in the Supporting Information revealed an essentially equivalent Pd size (ca. 2.5 nm) for the 400 °C treated Pd/XC-72-HNO_3 samples. These facts, together with the evidently enhanced activity registered for the similarly post-heat-treated Pd catalysts loaded on other carbon nanostructures (Table S2 in the Supporting Information), strongly favor the suggestion that the hydrophobicity of the underlying support is one of the key factors in contributing to the observed high activity.

Having demonstrated the superiority of the surface modulation approach, we sought to further elucidate the fundamental aspects underlying the wettability-driven phenomenon. Considering that water is also involved in **1b** formation, an additional set of experiments focused on examining the dependence of **1a** conversion on H_2O concentration was undertaken. As opposed to the trends observed with **1a** concentration, the reaction rate was found to be H_2O insensitive for both Pd/XC-72-700-Ar and Pd/XC-72-HNO_3 samples (Figure S9 in the Supporting Information). Coupled with the inherently low kinetic isotope k_H/k_D value of only ca. 1.1−1.2 observed for the reaction of **1a** with H_2O and D_2O at 25 °C (Table S4 in the Supporting Information), these results indicate that the activation of H_2O is extremely facile, whereas the Si−H cleavage could be relatively slow.[10b] This is especially the case when the surface of the catalyst is hydrophilic in nature. Therefore, it seems that a favorable interaction between the organosilane molecules and the underlying hydrophobic support can provide a unique driving force to significantly decrease the activation barriers associated with silane activation during the **1a** transformation.

On a Pd-decorated hydrophobic surface, an excess of surface metal coverage may disfavor the adsorption of silanes at the microenvironment surrounding the Pd NPs, thereby resulting in lower catalytic activities. In this sense, a Pd loading of 1.0 wt % on XC-72-700-Ar was beneficial to a cooperative metal−support interaction, as shown in Figure S12 in the Supporting Information. It was also noticed that a polar solvent (i.e., THF) played an important role in ensuring good miscibility of the organosilanes with water (Figure S13 in the Supporting Information). In comparison with Pt, Ru, Rh, and Ir NPs supported on XC-72-700-Ar as reference catalysts, Pd on hydrophobic CB showed a unique activity for silane hydrolysis (Table S6 in the Supporting Information), thereby stressing the indispensable role of metallic Pd in facilitating the crucial Si−H activation under conditions relevant to dehydrogenative silylation. Meanwhile, Pd catalysts supported on conventional solid oxides showed very poor performance under identical conditions (Table S6, entries 5−8), thereby showing that the coupling of XC-72-700-Ar with Pd is essential for achieving a high dehydrocoupling activity. Note that the use of hydrophobically modified TiO_2 (P25) and Al_2O_3 as supports resulted in markedly enhanced dehydrocoupling activities (Table S6, entries 9 and 10), further confirming that surface hydrophobicity is imperative for this reaction system. Nevertheless, in view of the significantly lower performance levels associated with the hydrophobically modified mineral oxide supported systems, it is likely that the modification of the electronic properties of surface-anchored Pd by the underlying support might also contribute to the enhanced silane activation observed in the Pd- decorated CB materials.

Pd/XC-72-700-Ar also showed high activity for hydrolytic oxidation of various organosilanes (Table 2). In this sense, trialkylsilanes and aromatic silanes were effectively oxidized to their corresponding silanols without the formation of any disiloxane products. It was noted that the reactions involving less sterically hindered trialkylsilanes proceeded significantly faster in comparison to their bulky counterparts (Table 2, entries 1 and 4). The same reactivity trend was also observed upon increasing the number of phenyl substituents on the organosilanes (Table 2, entries 5−7). Remarkably, we attempted the oxidation of sterically hindered triisopropylsilane, which is well-known to be problematic (i.e., it requires either an extensive reaction time of 24 h[10d] or a low S/C ratio of 33[10e]). In our case, a significantly shorter time of 20 min with a high S/C ratio of 2500 was sufficient for the reaction until completion. In addition, considerably higher organosilanol yields were also obtained (via conversion of triphenylsilane into triphenylsilanol) for Pd/XC-72-700-Ar (99%, 60 min) in comparison to the previously reported supported gold catalyst (28%, 24 h).[10d]

Table 2. Dehydrocoupling of Various Silanes and H_2O over 1.0 wt % Pd/XC-72-700-Ar[a]

$$R_{(4-n)}Si{-}H_n + n\,H_2O \rightarrow R_{(4-n)}Si{-}(OH)_n + n\,H_2$$

entry	silane	time (min)	yield (%)	TOF (h^{-1})[b]
1	Et_3SiH	1	>99	645300
2	Et_2SiH_2	6	90	97700
3[c]	$(i\text{-Pr})_3SiH$	21	98	7164
4	$(n\text{-Bu})_3SiH$	2.4	98	263500
5	$PhMe_2SiH$	3	99	213200
6	Ph_2MeSiH	23	98	27500
7[c]	Ph_3SiH	60	99	2482
8[d]	Et_3SiH	15	99	628400

[a]Reaction conditions unless specified otherwise: 5 mmol of silane, 0.5 mL of water, 10 mL of THF, S/C = 10000, air atmosphere, 25 °C. [b]Based on total Pd atoms. [c]S/C = 2500. [d]Reaction conditions; 50 mmol of **1a**, 5 mL of water, 100 mL of THF, S/C = 80000, air atmosphere, 25 °C.

DOI: 10.1021/acscatal.6b03233
ACS Catal. 2017, 7, 1720−1727

Given the superb reactivity observed for Pd/XC-72-700-Ar toward silane hydrolysis, we were curious to check whether this hydrophobically driven Pd catalysis would also allow for the dehydrogenative condensation of organosilanes with alcohols. As an alternative method for the synthesis of valuable silyl ethers, this transformation has recently attracted considerable attention[9d,14] because of its critical advantage over the conventional etherification method, which suffers from several drawbacks associated with the use of chlorosilanes[15] or disilazanes.[16] The results presented in Table 3 indicate that it

Table 3. Production of Various Silyl Ethers via Dehydrocoupling of 1a and Alcohol[a]

$$n\,Et_3Si{-}H\,(\mathbf{1a}) + R(OH)_n \rightarrow (Et_3Si{-}O)_nR + n\,H_2$$

entry	alcohol	time (min)	yield (%)	TOF (h^{-1})[b]
1	MeOH	1	>99	619300
2	EtOH	2.7	>99	230400
3	*i*-PrOH	25	>99	24930
4	*n*-BuOH	3	>99	208100
5	benzyl alcohol	1.8	99	346500
6[c]	ethylene glycol	3	96	48230
7[d]	glycerol	35	94	4101
8[e]	MeOH	53	99	11570

[a]Reaction conditions unless specified otherwise: 20 mmol of **1a**, 30 mmol of alcohol, 1.0 wt % Pd/XC-72-700-Ar, S/C = 10000, air atmosphere, 25 °C. [b]Based on total Pd atoms. [c]Reaction conditions: 10 mmol of alcohol, S/C = 2500. Yield refers to the disilylation product. [d]Reaction conditions: 6.7 mmol of alcohol, S/C = 2500, 60 °C. Yield refers to the trisilylation product. [e]Reaction conditions: 1.0 wt % Pd/XC-72-HNO_3.

is possible to achieve direct dehydrogenative alcoholysis of the organosilanes in pure alcohols, with the efficiency of this process being essentially comparable to that of silane hydrolysis. For example, at an S/C ratio of 10000, the silyl ether produced from **1a** and MeOH was exclusively obtained over a period of 1 min at 25 °C (corresponding to a TOF of $6 \times 10^5\ h^{-1}$ for alcohol silylation, entry 1). Note that polyalcohols such as ethylene glycol and glycerol, which can be derived from biomass,[17] were also suitable substrates for this etherification (entries 6 and 7), thereby further substantiating the utility of this approach for Si−O−C bond construction together with on-demand H_2 generation.

Dehydrogenative condensation of organosilanes and amines also represents one of the most attractive and atom-economical synthetic approach to access silylamines, an important class of silicon compounds that have been widely used as silylation agents, ligands for organometallic compounds, and precursors for Si and N polymeric materials.[18] Both homogeneous and heterogeneous catalysts have been reported for this reaction,[19] although control of the selectivity for Si−N coupling has proved to be challenging, as the reaction can lead to several products with different Si/N ratios (e.g., polysilazanes) as a result of multiple dehydrocoupling steps. Remarkably, we found that Pd/XC-72-700-Ar can robustly and selectively furnish the desired silylamines (Scheme 1), with activities (TOF) being orders of magnitude higher in comparison to those of previously employed catalysts for this transformation.[19b,c,j] As in the case of hydrolytic and alcoholic oxidations of organosilanes (see Tables 1 and 3), the hydrophobic Pd/XC-72-700-Ar catalyst persistently showed a boosted efficiency in comparison to its hydrophilic counterpart (Table S7 in the

Scheme 1. Production of Various Silylamines via Dehydrocoupling of 1a and Amines over 1.0 wt % Pd/XC-72-700-Ar[a]

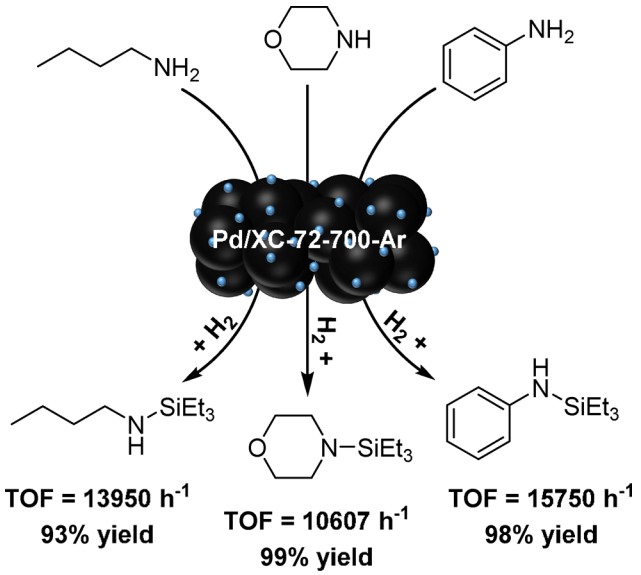

[a]Reaction conditions: 5 mmol of **1a**, 5 mmol of amine, 5 mL of dried THF, S/C = 2500, Ar atmosphere, 60 °C.

Supporting Information). To the best of our knowledge, this hydrophobically driven catalysis represents the most efficient, simple, and eco-friendly catalytic system to date, achieving convenient and controlled organosilane aminolysis (Table S10 in the Supporting Information).

3. CONCLUSIONS

In summary, the hydrophobic characteristics of the underlying supports were favorably utilized for boosting the efficiency of Pd NPs catalyzed dehydrogenative coupling of organosilanes. The catalytic activities obtained for these dehydrogenative silylation reactions were, to our knowledge, the highest reported to date. Our results revealed the key role of the surface wettability modulation in maximizing the performance of supported noble metals under catalytically relevant conditions. While the reported system holds promise for the development of a practical dehydrogenative silylation technology based on Si−H activation, we believe that careful tuning of the support wettability to meet reaction requirements will open a new avenue for heterogeneous catalysis processes mediated by supported metals.

4. EXPERIMENTAL SECTION

4.1. Hydrolysis of Organosilanes in an Open System.

All catalytic experiments were carried out in an ambient atmosphere of air; unless otherwise stated, the reactions were performed in a double-walled thermostatically controlled reaction vessel with a reflux condenser, which was connected to an automatic gas buret, where the gases were collected. Silane and H_2O (or D_2O) were mixed with 10 mL of THF in a reaction vessel under steady magnetic stirring (800 rpm) at given temperature (17−33 °C). The reaction was started by the addition of a certain amount of catalyst. In addition, evolved gas was qualitatively and quantitatively analyzed by an Agilent 6820 GC equipped with a TDX-01 column connected to a TCD. The catalyst was centrifuged, and the yield of the corresponding

DOI: 10.1021/acscatal.6b03233
ACS Catal. 2017, 7, 1720−1727

organosilanol was analyzed by an Agilent 7820A GC equipped with an HP-5 column connected to an FID using ethylbenzene as an internal standard. Identification of the products was performed by using a GC-MS spectrometer. The initial TOF was calculated on the organosilane conversion at 15%.

4.2. Generation of Hydrogen on Demand using 1 wt % Pd/XC-72-700-Ar as Catalyst. H_2O (2.5 mL) and Pd/XC-72-700-Ar (S/C = 2500) were mixed with 50 mL of THF in a two-neck flask with steady magnetic stirring (800 rpm) at 25 °C, which was connected to an automatic gas buret. The flask was sealed with an injector connected to an injection pump. For the stepwise hydrolysis process, **1a** (25 mmol) was sequentially injected into the flask at intervals until it was fully consumed. For the continuously controllable hydrolysis process, **1a** (25 mmol) was continuously injected into within 27 min until it was fully consumed. In addition, the evolved gas was qualitatively and quantitatively analyzed by an Agilent 6820 GC equipped with a TDX-01 column connected to a TCD.

4.3. Large-Scale Durability of 1 wt % Pd/XC-72-700-Ar Catalyst for Hydrolysis of 1a. **1a** (50 mmol) and water (5 mL) were mixed with 100 mL of THF in a reaction vessel (250 mL) with steady magnetic stirring (800 rpm) at 25 °C, which was connected to an automatic gas buret. The reaction was started by the addition of Pd/XC-72-700-Ar (S/C = 80000). After the reaction was complete, the centrifuged catalysts from parallel activity tests were collected and washed with distilled water, followed by drying in air at 100 °C for 12 h. All catalytic activity tests were repeatedly carried out by following the same procedure as described above.

4.4. Triethylsilane Adsorption Ability of Various Supports. Various supports (0.5 g) were placed in a Schlenk tube and pretreated at 150 °C under outgassing for 30 min, followed by the addition of **1a** (5 mmol), H_2O (0.5 mL), and THF (10 mL). Then the mixtures were stirred at 25 °C for 30 min in an ambient atmosphere of air. The adsorption amounts were determined by changes in **1a** concentration monitored by GC using ethylbenzene as an internal standard according to a previous report.[20]

4.5. Alcoholysis of Organosilanes in an Open System. **1a** (20 mmol) and alcohol were mixed in a reaction vessel with steady magnetic stirring (800 rpm) at a given temperature in an air atmosphere, which was connected to an automatic gas buret. The reaction was started by the addition of a certain amount of catalyst. In addition, the evolved gas was qualitatively and quantitatively analyzed by an Agilent 6820 GC equipped with a TDX-01 column connected to a TCD. The catalyst was centrifuged, and the yield of the corresponding silyl ether was analyzed by an Agilent 7820A GC equipped with an HP-5 column connected to an FID using bibenzyl as an internal standard. Identification of the products was performed by NMR analyses. The initial TOF was calculated on the organosilane conversion at 15%.

4.6. Aminolysis of Organosilanes in an Open System. **1a** (5 mmol), amine (5 mmol), dried THF (5 mL), and a certain amount of catalyst were mixed in a reaction vessel with steady magnetic stirring (800 rpm) at 60 °C under an argon atmosphere with a reflux condenser, which was connected to a drying tube and an automatic gas buret. In addition, the evolved gas was qualitatively and quantitatively analyzed by an Agilent 6820 GC equipped with a TDX-01 column connected to a TCD. The catalyst was centrifuged, and the yield of the corresponding silylamine was analyzed by an Agilent 7820A GC equipped with an HP-5 column connected to an FID using naphthalene as an internal standard. The product was isolated by distillation and identified by NMR analyses. The initial TOF was calculated on the organosilane conversion at 15%.

4.7. Characterization. The metal loading was measured by inductively coupled plasma atomic emission spectroscopy (ICP-AES) using a Thermo Electron IRIS Intrepid II XSP spectrometer. The BET specific surface areas of the prepared catalysts were determined by adsorption−desorption of nitrogen at liquid nitrogen temperature, using a Micromeritics TriStar 3000 instrument. Sample degassing was carried out at 300 °C prior to acquiring the adsorption isotherm. The crystal structures were characterized with X-ray diffraction (XRD) on a Bruker D8 Advance X-ray diffractometer using the Ni-filtered Cu Kα radiation source at 40 kV and 40 mA. XPS data were recorded with a PerkinElmer PHI 5000C system equipped with a hemispherical electron energy analyzer. The spectrometer was operated at 15 kV and 20 mA, and a magnesium anode (Mg Kα, $h\nu$ = 1253.6 eV) was used. The C 1s line (284.6 eV) was used as the reference to calibrate the binding energies (BE). Fourier transform infrared spectroscopy (FT-IR) was carried out with a Nicolet iS10 FT-IR spectrometer equipped with a DTGS detector, in the range 400−4000 cm^{-1}, by applying an optical resolution of 0.4 cm^{-1}. The samples were investigated by using the KBr pellet technique. A JEOL 2011 microscope operating at 200 kV equipped with an EDX unit (Si(Li) detector) was used for the TEM investigations. The samples for electron microscopy were prepared by grinding and subsequent dispersing of the powder in ethanol and applying a drop of a very dilute suspension on a carbon-coated grid. The size distribution of the metal nanoparticles was determined by measuring about 200 random particles in the images. *n*-Hexane or H_2O adsorption experiments were performed at 25 °C on a BEL SORP-max adsorption instrument. The adsorption amount of *n*-hexane or H_2O was recorded at the saturated vapor pressure of *n*-hexane (25 °C, 20.16 KPa) or H_2O (25 °C, 3.169 KPa). The Pd surface area was measured by CO chemisorptions using an AutoChem HP 2950 apparatus with a quantitative loop from Micromeritics. The sample was first pretreated with 5 vol % H_2/Ar at 200 °C for 2 h, and then pure CO was pulsed over the sample at 25 °C several times to saturated adsorption. The total amount of CO adsorbed was measured by assuming a chemisorption stoichiometry of CO/Pd = 1 and a Pd surface atomic density of 1.27×10^{19} m^{-2}.[21] The dispersion (D) was calculated according to the formula D = (surface number of Pd atoms)/(total number of Pd atoms).

■ ASSOCIATED CONTENT

Supporting Information

The Supporting Information is available free of charge on the ACS Publications website at DOI: 10.1021/acscatal.6b03233.

Experimental details of the catalyst preparation, TEM data, FT-IR data, adsorption capacity study, XPS data, optimization of reaction conditions, kinetic experiments, spectral parameters, and NMR data of products (PDF)

■ AUTHOR INFORMATION

Corresponding Authors

*E-mail for Y.C.: yongcao@fudan.edu.cn.

*E-mail for Y.-D.W.: wangyd.sshy@sinopec.com.

ORCID

Yong Cao: 0000-0002-8333-0181

DOI: 10.1021/acscatal.6b03233
ACS Catal. 2017, 7, 1720−1727

Notes

The authors declare no competing financial interest.

■ ACKNOWLEDGMENTS

This work was supported by the National Natural Science Foundation of China (21273044, 21473035, 91545108), the Science & Technology Commission of Shanghai Municipality (16ZR1440-400), SINOPEC (X514005), and the Open project of State Key Laboratory of Chemical Engineering (SKL-ChE-15C02).

■ REFERENCES

(1) (a) Dumesic, J. A.; Huber, G. W.; Boudart, M. In *Handbook of Heterogeneous Catalysis*; Ertl, G., Knozinger, H., Schüth, F., Weitkamp, J., Eds.; Wiley-VCH: Weinheim, Germany, 2008; Vol. *1*, pp 1−3. (b) Busca, G. *Heterogeneous Catalytic Materials: Solid State Chemistry, Surface Chemistry and Catalytic Behaviour*; Elsevier: Amsterdam, 2014; pp 1−7. (c) Munnik, P.; de Jongh, P. E.; de Jong, K. P. *Chem. Rev.* **2015**, *115*, 6687−6718.

(2) (a) Wang, M.; Wang, F.; Ma, J.; Chen, C.; Shi, S.; Xu, J. *Chem. Commun.* **2013**, *49*, 6623−6625. (b) Wang, L.; Xiao, F. S. *ChemCatChem* **2014**, *6*, 3048−3052. (c) Dai, Y.; Liu, S.; Zheng, N. *J. Am. Chem. Soc.* **2014**, *136*, 5583−5586.

(3) Bhaumik, A.; Mukherjee, P.; Kumar, R. *J. Catal.* **1998**, *178*, 101−107.

(4) (a) Corma, A.; Esteve, P.; Martínez, A. *J. Catal.* **1996**, *161*, 11−19. (b) Jing, H.; Guo, Z.; Ma, H.; Evans, D. G.; Duan, X. *J. Catal.* **2002**, *212*, 22−32. (c) Gounder, R.; Davis, M. E. *J. Catal.* **2013**, *308*, 176−188.

(5) (a) Li, C.-J. *Acc. Chem. Res.* **2009**, *42*, 335−344. (b) Scheuermann, C. J. *Chem. - Asian J.* **2010**, *5*, 436−451.

(6) (a) Brown, J. F.; Vogt, L. H. *J. Am. Chem. Soc.* **1965**, *87*, 4313. (b) Murugavel, R.; Voigt, A.; Walawalkar, M. G.; Roesky, H. W. *Chem. Rev.* **1996**, *96*, 2205−2536. (c) Li, G.; Wang, L.; Ni, H.; Pittman, C. U. *J. Inorg. Organomet. Polym.* **2001**, *11*, 123−154. (d) Jeon, M.; Han, J.; Park, J. *ACS Catal.* **2012**, *2*, 1539−1549.

(7) (a) Murahashi, S.-I.; Komiya, N.; Terai, H. *Angew. Chem., Int. Ed.* **2005**, *44*, 6931−6933. (b) Murahashi, S.-I.; Nakae, T.; Terai, H.; Komiya, N. *J. Am. Chem. Soc.* **2008**, *130*, 11005−11012. (c) Murahashi, S.-I.; Komiya, N.; Terai, H.; Nakae, T. *J. Am. Chem. Soc.* **2003**, *125*, 15312−15313. (d) Brasche, G.; Buchwald, S. L. *Angew. Chem., Int. Ed.* **2008**, *47*, 1932−1934.

(8) Walsh, R. *Acc. Chem. Res.* **1981**, *14*, 246−252.

(9) (a) Lee, M.; Ko, S.; Chang, S. *J. Am. Chem. Soc.* **2000**, *122*, 12011−12012. (b) Ison, E. A.; Corbin, R. A.; Abu-Omar, M. M. *J. Am. Chem. Soc.* **2005**, *127*, 11938−11939. (c) Tan, S. T.; Kee, J. W.; Fan, W. Y. *Organometallics* **2011**, *30*, 4008−4013. (d) Sattler, W.; Parkin, G. *J. Am. Chem. Soc.* **2012**, *134*, 17462−17465. (e) Kikukawa, Y.; Kuroda, Y.; Yamaguchi, K.; Mizuno, N. *Angew. Chem., Int. Ed.* **2012**, *51*, 2434−2437. (f) Yu, M.; Jing, H.; Fu, X. *Inorg. Chem.* **2013**, *52*, 10741−10743. (g) Teo, A. K. L.; Fan, W. Y. *Chem. Commun.* **2014**, *50*, 7191−7194. (h) Garcés, K.; Fernández-Alvarez, F. J.; Polo, V.; Lalrempuia, R.; Pérez-Torrente, J. J.; Oro, L. A. *ChemCatChem* **2014**, *6*, 1691−1697. (i) Yu, M.; Jing, H.; Liu, X.; Fu, X. *Organometallics* **2015**, *34*, 5754−5758. (j) Yap, C. P.; Poh, H. T.; Fan, W. Y. *RSC Adv.* **2016**, *6*, 5903−5906.

(10) (a) Jeon, M.; Han, J.; Park, J. *ChemCatChem* **2012**, *4*, 521−524. (b) Shimizu, K.-i.; Kubo, T.; Satsuma, A. *Chem. - Eur. J.* **2012**, *18*, 2226−2229. (c) Kamachi, T.; Shimizu, K.-i.; Yoshihiro, D.; Igawa, K.; Tomooka, K.; Yoshizawa, K. *J. Phys. Chem. C* **2013**, *117*, 22967−22973. (d) Mitsudome, T.; Noujima, A.; Mizugaki, T.; Jitsukawa, K.; Kaneda, K. *Chem. Commun.* **2009**, 5302−5304. (e) Asao, N.; Ishikawa, Y.; Hatakeyama, N.; Menggenbateer; Yamamoto, Y.; Chen, M.; Zhang, W.; Inoue, A. *Angew. Chem., Int. Ed.* **2010**, *49*, 10093−10095. (f) John, J.; Gravel, E.; Hagège, A.; Gacoin, H.; Li, T.; Doris, E. *Angew. Chem., Int. Ed.* **2011**, *50*, 7533−7536. (g) Li, W.; Wang, A.; Yang, X.; Huang, Y.; Zhang, T. *Chem. Commun.* **2012**, *48*, 9183−9185. (h) Liu, T.; Yang, F.; Li, Y.; Ren, L.; Zhang, L.; Xu, K.; Wang, X.; Xu, C.; Gao, J. *J. Mater. Chem. A* **2014**, *2*, 245−250. (i) Wang, Y.; Wan, X.-K.; Ren, L.; Su, H.; Li, G.; Malola, S.; Lin, S.; Tang, Z.; Häkkinen, H.; Teo, B. K.; Wang, Q.-M.; Zheng, N. *J. Am. Chem. Soc.* **2016**, *138*, 3278−3281. (j) Mitschang, F.; Schmalz, H.; Agarwal, S.; Greiner, A. *Angew. Chem., Int. Ed.* **2014**, *53*, 4972−4975. (k) Villemin, E.; Gravel, E.; Jawale, D. V.; Prakash, P.; Namboothiri, I. N. N.; Doris, E. *Macromol. Chem. Phys.* **2015**, *216*, 2398−2403. (l) Mitsudome, T.; Arita, S.; Mori, H.; Mizugaki, T.; Jitsukawa, K.; Kaneda, K. *Angew. Chem., Int. Ed.* **2008**, *47*, 7938−7940. (m) Kisukuri, C. M.; Palmeira, D. J.; Rodrigues, T. S.; Camargo, P. H. C.; Andrade, L. H. *ChemCatChem* **2016**, *8*, 171−179. (n) Saito, A.; Kinoshita, H.; Shimizu, K.-i.; Nishina, Y. *Bull. Chem. Soc. Jpn.* **2016**, *89*, 67−73.

(11) (a) Yadav, M.; Akita, T.; Tsumori, N.; Xu, Q. *J. Mater. Chem.* **2012**, *22*, 12582−12586. (b) Zhao, E. W.; Zheng, H.; Ludden, K.; Xin, Y.; Hagelin-Weaver, H. E.; Bowers, C. R. *ACS Catal.* **2016**, *6*, 974−978. (c) Zhou, Y.; Li, Y.; Shen, W. *Chem. - Asian J.* **2016**, *11*, 1470−1488.

(12) (a) Donnet, J.-B.; Voet, A. *Carbon Black-Physics, Chemistry and Elastomer Reinforcement*; Marcel Dekker: New York, 1976; pp 1−362. (b) Donnet, J.-B.; Bansal, R. C.; Wang, M. J. *Carbon Black-Science and Technology*, 2nd ed.; Marcel Dekker: New York, 1993; pp 1−461. (c) Sosa, R. C.; Masy, D.; Rouxhet, P. G. *Carbon* **1994**, *32*, 1369−1375.

(13) (a) Bi, Q. Y.; Lin, J. D.; Liu, Y. M.; Du, X. L.; Wang, J. Q.; He, H. Y.; Cao, Y. *Angew. Chem., Int. Ed.* **2014**, *53*, 13583−13587. (b) Zhu, Q. L.; Tsumori, N.; Xu, Q. *J. Am. Chem. Soc.* **2015**, *137*, 11743−11748. (c) Bi, Q. Y.; Lin, J. D.; Liu, Y. M.; He, H. Y.; Huang, F. Q.; Cao, Y. *Angew. Chem., Int. Ed.* **2016**, *55*, 11849−11853.

(14) (a) Sommer, L. H.; Lyons, J. E. *J. Am. Chem. Soc.* **1967**, *89*, 1521−1522. (b) Hara, K.; Akiyama, R.; Takakusagi, S.; Uosaki, K.; Yoshino, T.; Kagi, H.; Sawamura, M. *Angew. Chem., Int. Ed.* **2008**, *47*, 5627−5630. (c) Taguchi, T.; Isozaki, K.; Miki, K. *Adv. Mater.* **2012**, *24*, 6462−6467. (d) Mitsudome, T.; Yamamoto, Y.; Noujima, A.; Mizugaki, T.; Jitsukawa, K.; Kaneda, K. *Chem. - Eur. J.* **2013**, *19*, 14398−14402. (e) Blandez, J. F.; Primo, A.; Asiri, A. M.; Álvaro, M.; García, H. *Angew. Chem., Int. Ed.* **2014**, *53*, 12581−12586. (f) Dhakshinamoorthy, A.; Concepcion, P.; García, H. *Chem. Commun.* **2016**, *52*, 2725−2728. (g) Luo, X. L.; Crabtree, R. H. *J. Am. Chem. Soc.* **1989**, *111*, 2527−2535. (h) Ojima, Y.; Yamaguchi, K.; Mizuno, N. *Adv. Synth. Catal.* **2009**, *351*, 1405−1411. (i) Peterson, E.; Khalimon, A. Y.; Simionescu, R.; Kuzmina, L. G.; Howard, J. A. K.; Nikonov, G. I. *J. Am. Chem. Soc.* **2009**, *131*, 908−909. (j) Mukherjee, D.; Thompson, R. R.; Ellern, A.; Sadow, A. D. *ACS Catal.* **2011**, *1*, 698−702. (k) Fukumoto, K.; Kasa, M.; Nakazawa, H. *Inorg. Chim. Acta* **2015**, *431*, 219−221. (l) Toutov, A. A.; Betz, K. N.; Haibach, M. C.; Romine, A. M.; Grubbs, R. H. *Org. Lett.* **2016**, *18*, 5776−5779.

(15) Hatano, B.; Toyota, S.; Toda, F. *Green Chem.* **2001**, *3*, 140−142.

(16) (a) Firouzabadi, H.; Iranpoor, N.; Amani, K.; Nowrouzi, F. *J. Chem. Soc. Perkin Trans. 1* **2002**, *1*, 2601−2604. (b) Kadam, S. T.; Kim, S. S. *J. Organomet. Chem.* **2009**, *694*, 2562−2566.

(17) Haveren, J. v.; Scott, E. L.; Sanders, J. *Biofuels, Bioprod. Biorefin.* **2008**, *2*, 41−57.

(18) (a) Armitage, D. A. In *The Silicon-Heteroatom Bond*; Patai, S., Rappoport, Z., Eds.; Wiley: Chichester, U.K., 1991; pp 365−446. (b) Hardwick, J. A.; Pavelka, L. C.; Baines, K. M. *Dalton Trans.* **2012**, *41*, 609−621.

(19) (a) Sommer, L. H.; Citron, J. D. *J. Org. Chem.* **1967**, *32*, 2470−2472. (b) Blandez, J. F.; Esteve-Adell, I.; Alvaro, M.; García, H. *Catal. Sci. Technol.* **2015**, *5*, 2167−2173. (c) Mitsudome, T.; Urayama, T.; Maeno, Z.; Mizugaki, T.; Jitsukawa, K.; Kaneda, K. *Chem. - Eur. J.* **2015**, *21*, 3202−3205. (d) Liu, X.; Wu, Z.; Peng, Z.; Wu, Y. D.; Xue, Z. *J. Am. Chem. Soc.* **1999**, *121*, 5350−5351. (e) Takaki, K.; Kamata, T.; Miura, Y.; Shishido, T.; Takehira, K. *J. Org. Chem.* **1999**, *64*, 3891−3895. (f) Gutsulyak, D. V.; Vyboishchikov, S. F.; Nikonov, G. I. *J. Am. Chem. Soc.* **2010**, *132*, 5950−5951. (g) Dunne, J. F.; Neal, S. R.; Engelkemier, J.; Ellern, A.; Sadow, A. D. *J. Am. Chem. Soc.* **2011**, *133*, 16782−16785. (h) Xie, W.; Hu, H.; Cui, C. *Angew. Chem., Int. Ed.* **2012**, *51*, 11141−11144. (i) Toh, C. K.; Poh, H. T.; Lim, C. S.; Fan, W. Y. *J. Organomet. Chem.* **2012**, *717*, 9−13. (j) Bellini, C.; Carpentier,

DOI: 10.1021/acscatal.6b03233
ACS Catal. 2017, 7, 1720−1727

J.-F.; Tobisch, S.; Sarazin, Y. *Angew. Chem., Int. Ed.* **2015**, *54*, 7679−7683. (k) Bellini, C.; Orione, C.; Carpentier, J.-F.; Sarazin, Y. *Angew. Chem., Int. Ed.* **2016**, *55*, 3744−3748. (l) Liao, Q.; Cavaillé, A.; Saffon-Merceron, N.; Mézailles, N. *Angew. Chem., Int. Ed.* **2016**, *55*, 11212−11216.

(20) Cychosz, A. K.; Wong-Foy, A. G.; Matzger, A. J. *J. Am. Chem. Soc.* **2008**, *130*, 6938.

(21) (a) Mahata, N. *J. Catal.* **2000**, *196*, 262−270. (b) Jones, S.; Qu, J.; Tedsree, K.; Gong, X. Q.; Tsang, S. C. E. *Angew. Chem., Int. Ed.* **2012**, *51*, 11275−11278.

DOI: 10.1021/acscatal.6b03233
ACS Catal. 2017, 7, 1720−1727